

## Spots and Plages: The Solar Perspective

Sami K. Solanki

*Institute of Astronomy, ETH-Zentrum, CH-8092 Zurich, Switzerland*

**Abstract.** Spots and plages are prominent markers of magnetic fields on the Sun and on other cool stars. Here a brief overview is given of their observed properties, with similarities and differences emphasized. The distribution of sunspot sizes is discussed in greater detail. An extrapolation from the solar to the stellar case is made. For active stars it provides a natural explanation for the larger spot areas that are deduced from the strength of molecular spectral lines than from Doppler imaging.

### 1. Introduction

The Sun is the only star whose surface can be resolved at high resolution. Solar observations thus provide a unique insight into the fine-scale structure of the magnetic field on cool stars and its manifestations. On the other hand, the Sun covers only a restricted parameter range compared to the sum of other cool stars. The importance of this interplay between the study of the Sun and stars was well understood by Brendan Byrne, as witnessed by his keen and typically critical, but always good humoured, interest in solar physics.

Sunspots and plages are manifestations of the solar magnetic field which, in the solar photosphere, is filamented into flux tubes. These possess diameters ranging from below the best current spatial resolution of roughly 200 km to over 50000 km. Sunspots and plages are brightness signatures of magnetic flux tubes, with sunspots being the largest and plages being composed of the smallest (called magnetic elements). The small tubes do not fill the whole solar surface in a plage, but rather only some fraction, typically 5–25%.

The brightness of individual flux tubes is a strong function of their size, as can be seen from Figure 1. Small flux tubes are bright (with a possible decrease of excess brightness for the very smallest), while larger ones are dark. Plages, being conglomerates of many small and bright flux tubes, are consequently bright. The dark flux tubes are subdivided into sunspots, which are composed of an umbra and a penumbra, and pores, naked umbrae which, however, are considerably brighter than the umbrae of mature sunspots (Sütterlin 1998). In general, pores are smaller, with diameters of 500–5000 km, whereas sunspots have diameters larger than approximately 4000 km. When discussing the brightness of sunspots we need to distinguish between the average over the whole spot (solid curve in Figure 1) and the umbral brightness (dot-dashed curve).

The second basic parameter of flux tubes is their field strength. In contrast to their brightness, however, the field strength inside the flux tubes (when averaged over their cross-section) is remarkably constant over the whole range of

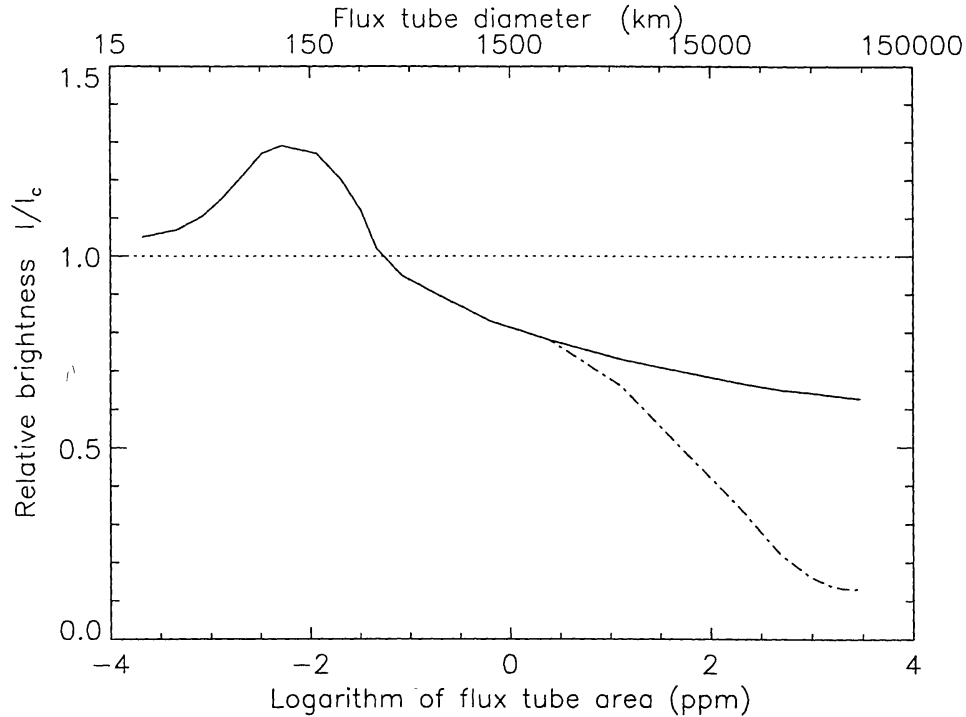


Figure 1. White-light brightness of magnetic features relative to ‘quiet’ Sun brightness vs. the (logarithmic) area of magnetic features in  $10^{-6}$  times the solar hemispheric area (lower axis) and their diameter (upper axis). The solid line represents the brightness averaged over the whole flux tube, i.e., over both umbra and penumbra for sunspots. The dot-dashed lines represents the brightness of the umbra only.

their sizes, as can be seen from Figure 2. Only the very smallest flux tubes show signs of a strongly reduced field strength (at the left edge of Figure 2, cf. § 5).

In the case of sunspots the field strength varies strongly over their cross-section, so that it is once again necessary to distinguish between the field strength averaged over the whole sunspot (solid curves in Fig. 2) and the *maximum* field strength in the umbra (dot-dashed curves).

## 2. Size Distribution of Solar Flux Tubes

Consider the question of the relative abundance of flux tubes of different sizes. Basically, the number of flux tubes rapidly increases with decreasing size, just as the number of bipolar magnetic regions rapidly increases with decreasing size or magnetic flux (Schrijver & Title 1999).

For sunspots this size distribution can be deduced from direct observations. Bogdan et al. (1988) considered the Mt Wilson sunspot areas measured between 1921 and 1982 and found that the distribution of umbral areas  $A$  larger than  $A_{\min} = 1.5 \times 10^{-6} A_{1/2\odot}$  (where  $A_{1/2\odot} = 2\pi R_{\odot}^2$  is the surface area of the visible solar hemisphere) is roughly described by a log-normal distribution, i.e., the number of sunspots  $N$  with umbral area  $A$  is given by

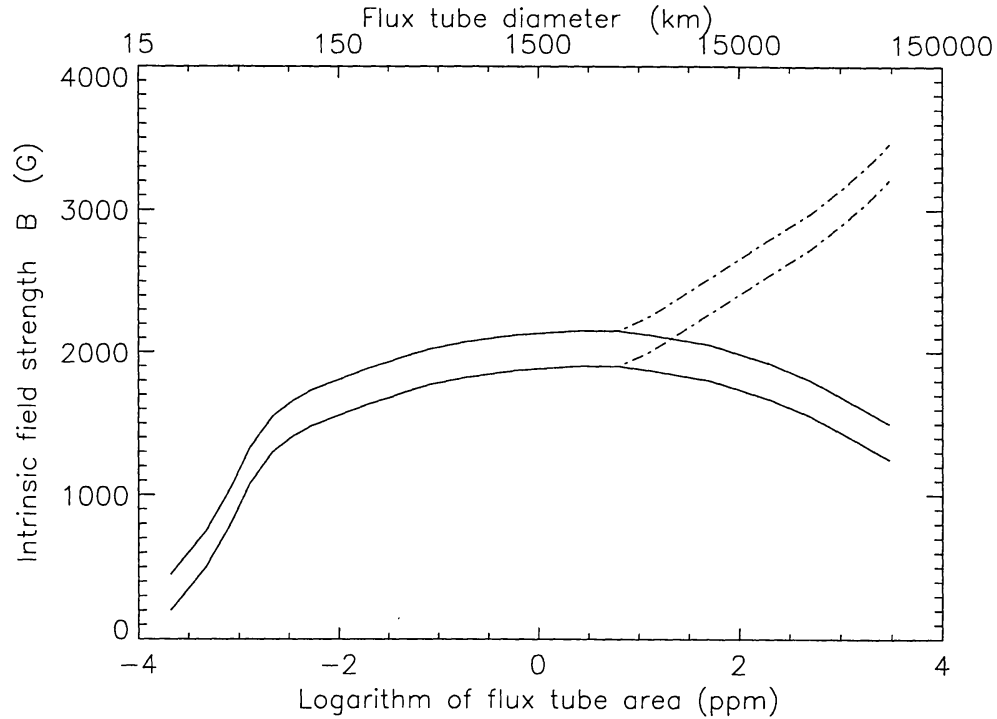


Figure 2. Intrinsic field strength  $B$  of magnetic features vs. the (logarithmic) area of magnetic features (lower axis, see Fig. 1) and their diameter (upper axis). The solid lines roughly enclose the observed range of values of the field strength averaged over the whole flux tube, including over both umbra and penumbra for sunspots. The dot-dashed lines represents the maximum field strength in the umbra.

$$\frac{dN}{dA} = \left(\frac{dN}{dA}\right)_{\max} \exp\left(-\frac{(\ln A - \ln \langle A \rangle)^2}{2 \ln \sigma_A}\right). \quad (1)$$

The distribution is characterized by three free parameters determined from the observations:  $(dN/dA)_{\max}$  is the maximum value reached by the distribution (for the Sun it is 9.2 in units of  $10^{-6} A_{1/2\odot}$ ),  $\langle A \rangle$  is the mean sunspot area ( $= 0.62$  in the same units) and  $\sigma_A$  is a measure of the width of the distribution ( $= 3.8$ ). The range of measured umbral diameters is approximately 1200–11500 km.

Bogdan et al. (1988) display the measured sunspot distributions for the three years around solar activity minimum and maximum (in their Figure 3), together with log-normal fits to them. The log-normal curves describing the sunspot distributions at solar maximum and minimum differ only in their  $(dN/dA)_{\max}$  values.

How does the distribution of flux-tube sizes continue to flux tubes with smaller diameters than those considered by Bogdan et al. (1988)? This question cannot be answered in a direct manner since area measurements become more and more unreliable as the flux-tube size decreases. Thus, no data sets of the

distribution of the area of even pores exist. Hence, the sizes and numbers are most uncertain for the smallest and most common magnetic elements.

Nevertheless, qualitative estimates can be made. Although individual magnetic elements (i.e., the small flux tubes composing plages) cannot be counted, the total plage area in active regions can easily be determined (note, however, that this includes the intervening space between the magnetic elements). It turns out that the ratio between the areas covered by plages and sunspots increases from approximately 12 at the maximum of the solar cycle to over 25 at solar activity minimum (Chapman et al. 1997). Hence, solar active-region plage covers *at least* an order of magnitude more of the surface area than sunspots. The above numbers are probably lower limits, since weaker, less bright plage regions are more easily missed than sunspots. Furthermore, magnetic elements also form the network, which is found on all parts of the ‘quiet’ Sun. If the network area is included in the above ratio then it probably varies between values of 20–30 and 50–60 over the solar cycle. Since only 10–20% of the surface area is covered by fields in a plage the amount of magnetic flux carried by plages and sunspots is on the same order of magnitude around activity maximum.

Indirect evidence that the surface area covered by magnetic elements is comparable to or larger than that covered by sunspots is also provided by the fact that the Sun seen as a star is brighter at times of high magnetic activity, i.e. at times when the number of sunspots on the solar surface is largest (e.g., Willson & Hudson 1988, 1991, Fröhlich & Lean 1998). Although the total irradiance (i.e., the wavelength-integrated flux as seen at the location of the Earth) varies by only 0.1–0.2% over the solar cycle, the measurements carried out from space are sufficiently accurate to detect it with ease.

Models which assume that only surface magnetism is the cause have been highly successful in reproducing the irradiance record (e.g., Foukal & Lean 1990, Chapman et al. 1996, Lean et al. 1998), and also a variety of other related diagnostics (Solanki & Unruh 1998, Fligge et al. 1998, Unruh et al. 1999). Hence, the brightening of the Sun at activity maximum is a direct result of the increased number of small flux tubes relative to large ones.

A particularly intriguing observation in this context is that whereas the brightness correlates directly with activity on solar-type stars with low activity levels (less than approximately three times the mean solar value), there is an anticorrelation for more active stars (Radick et al. 1989, Lockwood et al. 1992). This suggests that as the activity level rises, i.e. as the magnetic flux increases, the average size of magnetic flux tubes also increases. This is equivalent to saying that the number of larger flux tubes increases relative to smaller ones at higher activity levels.

In the following section I explore the consequences of a possible similar trend toward larger sunspots with increasing activity.

### 3. Extrapolation to more Active Stars

First consider the two functions  $dN/dA$  (given by Eq. 1) and  $A dN/dA$ , the latter of which describes the contribution of spots with area  $A$  to the total area covered by (sun)spots. The solar  $dN/dA$  and  $A dN/dA$  distributions are represented by the thick lines in Figure 3. Both functions have been normalized to their values

at  $A = 10$ . We evaluate numerically the integrals over both these distributions between  $A_{\min}$  and  $A$ . The second of these reads:

$$\int_{A_{\min}}^A A' \frac{dN}{dA'} dA' = \left( \frac{dN}{dA} \right)_{\max} \int_{A_{\min}}^A A' \exp \left( -\frac{(\ln A' - \ln \langle A \rangle)^2}{2 \ln \sigma_A} \right) dA'. \quad (2)$$

These integrals, computed using the values for  $\sigma_A$  and  $\langle A \rangle$  taken from Bogdan et al. (1988), are represented by the thick curves in Fig. 4. Plotted are  $S_N(A)$  and  $S_A(A)$ , i.e. the integrals normalized to their maximum values:

$$S_N(A) = \int_{A_{\min}}^A \frac{dN}{dA'} dA' / \int_{A_{\min}}^{A_{\max}} \frac{dN}{dA'} dA' = \int_{A_{\min}}^A dN / N_{\text{tot}}, \quad (3)$$

$$S_A(A) = \int_{A_{\min}}^A A' \frac{dN}{dA'} dA' / \int_{A_{\min}}^{A_{\max}} A' \frac{dN}{dA'} dA' = \int_{A_{\min}}^A A' dN / A_{\text{tot}}. \quad (4)$$

Figure 4 suggests that at least for the Sun small sunspots cover a far larger portion of the solar surface than larger sunspots. According to Figure 3 of Bogdan et al. (1988) the distribution of sunspot sizes is the same at activity maximum as at activity minimum. If on more active stars only  $dN/dA_{\max}$  would differ then the thick curve in Figure 4 would be valid for them as well, so that spots well below the resolution achievable with Doppler imaging would completely dominate the area coverage. In this case all spots on Doppler images would be (tight) clusters of many smaller spots.

A careful look at Figure 3 of Bogdan et al. (1988) does indicate that the distribution of the data points is somewhat flatter at activity maximum than at minimum. A flatter  $dN/dA$  curve can be achieved by increasing  $\sigma_A$ .

A flatter  $dN/dA$  curve implies that the  $A_{\text{tot}}/N_{\text{tot}}$  ratio is larger, since the increase in the number of larger sunspots produces a disproportionately larger increase in the spot area coverage. However, the change in shape between solar activity minimum and maximum is so small that we can expect:

$$\left( \frac{A_{\text{tot}}}{N_{\text{tot}}} \right)_{\text{solar max}} \lesssim 1.5 \left( \frac{A_{\text{tot}}}{N_{\text{tot}}} \right)_{\text{solar min}}. \quad (5)$$

Over the same period the total area covered by sunspots increases by a factor of almost 10. We then extrapolate to even larger activity levels by continuing to increase  $\sigma_A$  with increasing activity (or, equivalently, with increasing total sunspot area). The  $\sigma_A$  and total sunspot area coverage  $A_{\text{tot}}$  connected with the individual curves in Figures 3 and 4 are listed in Table 1 ( $A_{\text{tot}}$  is fixed such that  $A_{\text{tot}} \approx 3000$  around solar maximum, i.e. 0.3% of the visible hemisphere is covered by sunspots, in good agreement with observations published by, e.g., the Royal Greenwich Observatory). We have assumed that  $\sigma_A$  changes linearly with  $(dN/dA)_{\max}$ . Note that on the most active star in the table the spots cover

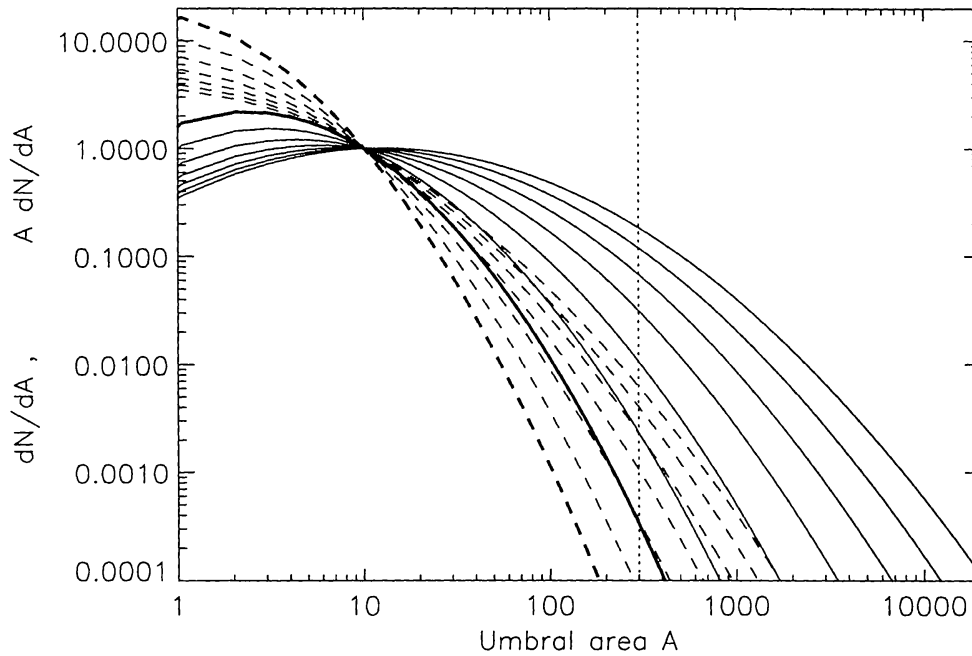


Figure 3. The distributions  $dN/dA$  (dashed curves) and  $A dN/dA$  (solid) vs. spot umbral area  $A$ . All distributions have been normalized to their values at  $A = 10$ . Thick curves represent solar activity minimum. The curves next to them correspond roughly to solar activity maximum. From left to right the plotted curves describe increased spottedness, i.e. increased stellar activity.

the whole stellar surface in this model (this corresponds to the rightmost curves in Figures 3 and 4).

Table 1: Parameters of Sun- and starspot distributions

solar:	min	max					
$\sigma_A$	3.8	5.0	6.8	9.2	12.2	15.8	20.0
$(dN/dA)_{\max}$	5	25	65	125	205	305	425
$A_{\text{tot}}$	80	760	4000	15170	46410	121110	250000
$A_{\text{spot,tot}}$	320	3000	16000	61000	186000	484000	$10^6$
$A_{\text{tot}}/N_{\text{tot}}$	5.0	7.4	11.6	18.0	27.3	39.7	55.7
$A_{\text{DI}}/A_{\text{tot}}$	0.0002	0.003	0.02	0.06	0.14	0.23	0.33

Accepting that good Doppler images for rapidly rotating stars can resolve spots  $5^\circ$  in longitude and assuming that spots are roughly round, we find that spot areas larger than 1200 in units of  $10^{-6}$  can be resolved (unless smaller spots appear in tight clumps). Assuming further that the ratio of umbral to penumbral area of 1:3 is independent of sunspot size means that spots with umbrae having



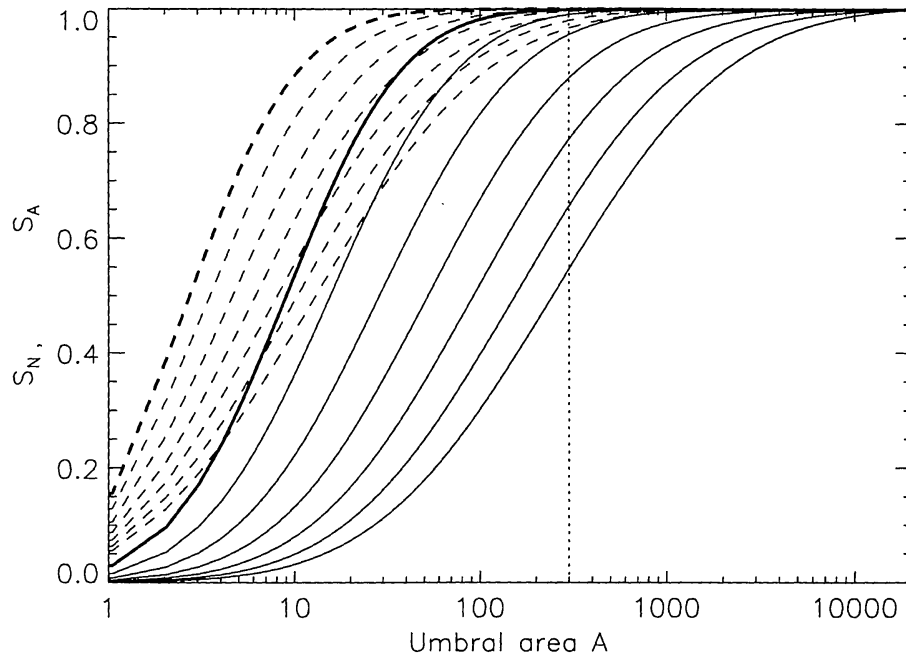


Figure 4. The integral functions  $S_N$  (dashed curves) and  $S_A$  (solid) vs. umbral area  $A$ .  $S_N$  and  $S_A$  are defined in the text.

areas above 300 can be resolved. This rough limit of resolvability is marked by the vertical dotted line in Figures 3 and 4.

The largest polar (or other) spots seen on Doppler Images of some very active stars cover up to 5–10% of the stellar hemisphere on dwarfs (e.g., Barnes et al. 1998, Strassmeier & Rice 1998) and on RS CVn subgiants (e.g., Vogt & Penrod 1983, Donati et al. 1992, Strassmeier 1997). This corresponds to  $A \approx 12000$ . Clearly, for the chosen form of the extrapolation (and the other assumptions of the current analysis) these large stellar spots are not single spots, but more likely are tight groups of smaller starspots.

If one now recalls that even the largest *sunspots* would not be resolved by even the highest resolution Doppler images this suggests that very likely in addition to the large spots seen on Doppler images of rapidly rotating stars a large number of smaller unresolved spots are present, which may well be more evenly distributed on the stellar surface and hence would not contribute to the Doppler image. This may provide an explanation for the fact that the spot filling factor derived from Doppler images (10–15%) is smaller than that obtained from the depths of molecular lines (30–50%; Neff et al. 1995, O’Neal et al. 1996, 1998).

The above conclusions depend on the various assumptions underlying the analysis. It is necessary to redo this analysis using other assumptions, which could influence the results.

#### 4. Properties of Sunspots

The large-scale magnetic structure of sunspots is straightforward, but on a small scale it has turned out to be rather complex. Basically, a sunspot as seen in white light is the intersection between a magnetic flux tube and the solar surface. The magnetic field is strongest and most vertical in the central, darkest part of the spot (maximum field strengths range from 2000 to 3500 G). It weakens and becomes more horizontal towards the outer boundary, where it is 700–1000 G and is inclined by 70–80° to the vertical. Beyond the visible edge of the sunspot the magnetic field forms a so-called canopy, composed of almost horizontal field lines overlying mainly field-free gas. The base of the canopy lies in the photosphere not too far from the sunspot boundary. In the penumbra the field is filamented, with most of the magnetic flux being in the form of field inclined by 40–70° to the vertical. However, a smaller proportion is in the form of thin, almost horizontal flux tubes. There is evidence that at least some of these horizontal flux tubes return into the solar interior at the sunspot boundary.

The Evershed effect, i.e. shifts of photospheric spectral lines showing a horizontal outflow of matter, is connected with these horizontal flux tubes. This material also returns to the solar interior at the sunspot boundary. Outflow velocities are typically a few km s<sup>-1</sup>. In the chromosphere and transition region a rapid inflow is observed (known as the inverse Evershed effect), which appears to follow the inclined magnetic field lines. Above the umbra it is seen mainly as a downflow that can be supersonic at transition-region temperatures (velocities vary between 5 km s<sup>-1</sup> and 100 km s<sup>-1</sup>; Kjeldseth-Moe et al. 1988, 1993). Nonetheless, the mass flux carried by the inverse Evershed flow is over an order of magnitude smaller than in the photospheric Evershed flow.

The magnetic field strength of sunspots is closely linked with their temperature (Kopp & Rabin 1992, Solanki et al. 1993, Martínez Pillet & Vázquez 1993). The relation between the two is, for relatively simple and unstressed sunspots, universal (with a small amount of scatter). Consequently, there is also an almost universal relation between the maximum field strength  $B_0$  and the minimum brightness of different sunspots. Both these quantities scale roughly linearly with the sunspot diameter (larger sunspots have darker umbrae; Kopp and Rabin 1992, Collados et al. 1994, Solanki 1997b). It has also been suggested that the intrinsic brightness of sunspots changes over the solar cycle (Albregtsen & Maltby 1978), with sunspot umbrae being approximately 17 % darker at the beginning of the solar cycle than at its end (in total flux, i.e. integrated over all wavelengths).

The temperature stratification of sunspot umbrae as compared to the ‘quiet’ Sun reveals that umbrae are significantly cooler only in photospheric and low chromospheric layers (e.g., Maltby et al. 1986; the comparison is made at equal optical depth or column mass. Due to the Wilson depression of 400–800 km a direct comparison at equal geometrical depth is problematic). In the upper chromosphere and lower transition region sunspots are distinctly hotter. The late chromospheric temperature rise and the higher chromospheric temperature give sunspots the distinctive Ca II H&K line profiles, with narrow, single peaked, but strong core reversals (Linsky & Avrett 1970).



In the transition region and corona the important quantity is the electron density at a given temperature, since most of the radiation is optically thin. The low umbral temperature in the photosphere implies that although the transition region above umbrae lies deeper than in the ‘quiet’ Sun (even after the Wilson depression is accounted for), the electron density at a given temperature is almost the same as in the ‘quiet’ Sun, as may be seen by comparing the various models of Maltby et al. (1986) with each other. This is the property directly responsible for the low umbral emissivity of X-rays and of transition-region line radiation (e.g., Harmon et al. 1993, Gurman 1993). Finally, however, this low emissivity implies that the heating per unit mass is not very different from the ‘quiet’ Sun value and certainly far lower than in plages.

## 5. Plages

Plages are the chromospheric and transition-region signature of particularly dense collections of small flux tubes. The corresponding brightenings in the photosphere are called faculae. The contrast relative to the ‘quiet’ Sun at wavelengths emanating in photospheric layers increases strongly towards the solar limb. The underlying flux tubes have diameters below approximately 500 km, with the smaller ones being bright at most wavelengths. The largest of the flux tubes forming plages are slightly dark in the continuum, but appear brighter (or neutral) in filtergrams taken in line cores or near the limb (cf. Sütterlin 1998, for a similar behaviour seen in pores).

Roughly 90% of the magnetic flux in plages is concentrated into these small flux tubes, which possess field strengths of 1500–1700 G at the solar surface (Rüedi et al. 1992, cf. Stenflo 1973): When expressed in terms of the plasma  $\beta = 8\pi p/B^2$ , where  $B$  is the field strength and  $p$  is the gas pressure within the flux tube, this implies that 90% of the magnetic flux has plasma  $\beta < 1$ . Hence, inside these flux tubes the magnetic field dominates energetically over the gas.

In the ‘quiet’ Sun not more than approximately half of the magnetic flux is in strong-field form (corresponding to  $\beta < 1$ , Meunier et al. 1998). A large fraction of the “weak field” is also in the form of flux tubes (field strength of 200–1000 G at the solar surface, Solanki et al. 1996). Hanle-effect measurements indicate that there is an even larger amount of flux hidden in the form of a turbulent field of 5–30 G (Faurobert-Scholl 1993; Faurobert-Scholl et al. 1995), i.e. a field that is tangled up on a small scale.

The thermal stratification of magnetic elements is largely responsible for the brightenings that characterize faculae and plages. Magnetic elements are hotter than the ‘quiet’ Sun at practically all heights in the solar atmosphere. The temperature contrast increases with height in the upper photosphere and higher layers, so that the brightness contrast increases rapidly towards shorter wavelength in the UV and is larger in spectral lines (the larger sensitivity of the Planck function to temperature at short wavelengths also plays a role). Two geometrical effects also help to determine the brightness of magnetic elements. Firstly, the magnetic elements expand with height, so that the *intensity* contrast in higher layers is larger even if the *temperature* contrast is not greater there. Secondly, magnetic features are partially evacuated, so that one sees deeper inside them (Wilson depression). The resulting hot walls are best visible away

from disc centre. This leads to an enhancement of photospheric emission from faculae near the limb of the sun (see Schüssler 1992 for a review).

In the upper atmosphere the brightness of plages is due to additional, non-radiative heating. Depending on the level in the atmosphere the dissipation of MHD waves (in the case of the chromosphere, Ulmschneider 1999) or magnetic reconnection (for the corona, Priest 1999) are the currently preferred modes of energy input. In either case the heating is driven by the dynamics of the magnetic flux tubes.

Relatively little is known of the internal dynamics of magnetic elements. The presence of stationary flows within the magnetic features is controversial. Evidence, both against steady flows (Solanki 1986, Stenflo & Harvey 1985, Frutiger & Solanki 1998) and for downflows (Bellot Rubio et al. 1997), has been presented. I favour the absence of such flows since then there is no need to worry about conserving mass inside the flux tube (a steady downflow would rapidly drain the corona due to the exponential decrease of the gas density with height).

Oscillations and waves in flux tubes have been intensively studied theoretically (e.g., Roberts & Ulmschneider 1997), but are difficult to observe (e.g., Solanki 1997a). There is evidence for low amplitude magneto-acoustic waves both below and above their cutoff frequency, which determines whether they propagate or not. There exists also indirect evidence for much larger amplitude non-stationary velocities (from, e.g., line widths). Magneto-acoustic and kink waves are the most likely sources of heating of the chromospheric layers of flux tubes (and hence of plages).

Finally, flux tubes are moved around as a whole due to the everchanging pattern of convective cells (the granulation). Thus each flux tube carries out a random walk on the solar surface. Since each flux tube is the footpoint of a bundle of field lines reaching up into the corona, such a random walk leads to the intertwining of field lines at greater heights. This in turn produces a build-up of magnetic energy and the formation of spontaneous current sheets and tangential discontinuities (Parker 1994). A part of this excess energy can be released through reconnection (Priest 1999, Schrijver & Title 1999).

Large flux tubes such as sunspots and pores are far less affected by the buffeting due to granulation in the sense that a smaller wave flux is excited. Random motions leading to braidings of field lines are also reduced. Consequently, the heating per unit mass of the chromosphere and coronae over larger flux tubes is reduced. This is the probable reason for the relatively small X-ray intensity exhibited by sunspot umbrae and pores.

More details on solar magnetic elements are given by Solanki (1993) and Steiner (1994).

**Acknowledgments.** It is a pleasure to thank Gerry Doyle and John Butler for the organization of this conference. Yvonne Unruh clarified a number of my questions concerning Doppler imaging and made many useful comments on the manuscript, which I gratefully acknowledge.

## References

Albregtsen F. & Maltby P., 1978, *Nature*, 274, 41

- Barnes J.R., Collier Cameron A., Unruh Y.C., Donati J.F. & Hussain G.A.J., 1998, , *Monthly Notices Royal Astron. Soc.* , 299, 904
- Bellot Rubio L.R., Ruiz Cobo B. & Collados M., 1997, ApJ, 478, L45
- Bogdan T.J., Gilman P.A., Lerche I. & Howard R., 1988, ApJ, 327, 451
- Chapman G.A., Cookson A.M. & Dobias J.J., 1996, , *J. Geophys. Res.* **101**, 13541
- Chapman G.A., Cookson A.M. & Dobias J.J., 1997, ApJ, 482, 541
- Collados M., Martínez Pillet V., Ruiz Cobo B., del Toro Iniesta J.C. & Vázquez M., 1994, A&A, 291, 622
- Donati J.-F., Brown S.F., Semel M., Rees D.E., Dempsey R.C., Mathews J.M., Henry G.W. & Hall D.S., 1992, A&A, 265, 682
- Faurobert-Scholl M., 1993, A&A, 268, 765
- Faurobert-Scholl M., Feautrier N., Machefert F., Petrovay K. & Spielfiedel A., 1995, A&A, 298, 289
- Fligge M., Solanki S.K., Unruh Y.C., Fröhlich C. & Wehrli Ch., 1998, A&A, 335, 709
- Foukal P. & Lean J., 1990, Science, 247, 556
- Fröhlich C. & Lean J., 1998, in *New Eyes to see inside the Sun and Stars*, F.-L. Deubner, J. Christensen-Dalsgaard, D. Kurtz (Eds.), Kluwer Academic Publ., Dordrecht, Netherlands, *IAU Symp.* **185**, 89
- Frutiger C. & Solanki S.K., 1998, A&A, 336, L65
- Gurman J.B., 1993, ApJ 412, 865
- Harmon R., Rosner R., Zirin H., Spiller E. & Golub L., 1993, ApJ, 417, L83
- Kjeldseth-Moe O., Brynildsen N., Brekke P., Engvold O., Maltby P., Bartoe J.-D.F., Brueckner G.E., Cook J.W., Dere K.P. & Soker D.G., 1988, ApJ, 334, 1066
- Kjeldseth-Moe O., Brynildsen N., Brekke P., Maltby P. & Brueckner G.E., 1993, *Solar Phys.*, 145, 257
- Kopp G. & Rabin D., 1992, *Solar Phys.*, 141, 253
- Lean J.L., Cook J., Marquette W., Johannesson A., 1998, ApJ, 492, 390
- Linsky J.L. & Avrett E.H., 1970, PASP, 82, 169
- Lockwood G.W., Skiff B.A., Baliunas S.L. & Radick R.R., 1992, Nature, 360, 653
- Maltby P., Avrett E.H., Carlsson M., Kjeldseth-Moe O., Kurucz R.L. & Loeser R., 1986, ApJ, 306, 284
- Martínez Pillet V. & Vázquez M., 1993, A&A, 270, 494
- Meunier N., Solanki S.K. & Livingston W., 1998, A&A, 331, 771
- Neff J.E., O'Neal D. & Saar S.H., 1995, ApJ, 452, 879
- O'Neal D., Saar S.H. & Neff J.E., 1996, ApJ, 463, 766
- O'Neal D., Saar S.H. & Neff J.E., 1998, ApJ, 501, L73
- Parker E.N., 1994, *Spontaneous current sheets in magnetic fields : with applications to stellar x-rays*, Oxford University Press, New York
- Priest E.R., 1999, these proceedings

- Radick R.R., Lockwood G.W. & Baliunas S.J., 1989, *Science*, 247, 39
- Roberts B. & Ulmschneider P., 1997, in *Solar and Heliospheric Plasma Physics*, C.E. Alissandrakis, G. Simnett & L. Vlahos (Eds.), Proc. 8th European Meeting on Solar Physics, Springer, Berlin, p. 75
- Rüedi I., Solanki S.K., Livingston W. & Stenflo, J.O., 1992, *A&A*, 263, 323
- Schrijver C.J. & Title, A.M., 1999, these proceedings
- Schüssler M., 1992, in *The Sun — a Laboratory for Astrophysics*, J.T. Schmelz, J.C. Brown (Eds.), Kluwer, Dordrecht, p. 191
- Solanki S.K., 1993, , *Space Sci. Rev.* , 61, 1
- Solanki S.K., 1986, *A&A*, 168, 311
- Solanki S.K., 1997a, in *Solar and Heliospheric Plasma Physics*, C.E. Alissandrakis, G. Simnett & L. Vlahos (Eds.), Springer, Berlin, p.49
- Solanki S.K., 1997b, in *Advances in the Physics of Sunspots*, B. Schmieder, J.C. del Toro Iniesta & M. Vázquez (Eds.), Astron. Soc. Pacific Conf. Ser., Vol. 118, p. 178
- Solanki S.K. & Unruh Y., 1998, *A&A*, 329, 747
- Solanki S.K., Walther U. & Livingston W., 1993, *A&A*, 277, 639
- Solanki S.K., Zuffrey D., Lin H., Rüedi I. & Kuhn J., 1996, *A&A*, 310, L33
- Steiner O., 1994, in *Infrared Solar Physics*, D. Rabin, J. Jefferies & C.A. Lindsey (Eds.), Kluwer, Dordrecht *IAU Symp.* , 154, 407
- Stenflo J.O., 1973, *Solar Phys.*, 32, 41
- Stenflo J.O. & Harvey J.W., 1985, *Solar Phys.*, 95, 99
- Strassmeier K.G. & Rice J.B., 1998, *A&A*, 330, 685
- Strassmeier K.G., 1997, *A&A*, 319, 535
- Sütterlin P., 1998 *A&A*, 333, 305
- Ulmschneider P., 1999, these proceedings.
- Unruh Y.C., Solanki S.K. & Fligge M., 1999, *A&A*, submitted
- Vogt S.S. & Penrod G.D., 1983, *PASP*, 95, 565
- Willson R.C. & Hudson H.S., 1988, *Nature*, 332, 810
- Willson R.C. & Hudson H.S., 1991, *Nature*, 351, 42